Period-one characteristic in an optoelectronic delayed feedback semiconductor laser and its application in sensing

Senlin Yan (颜森林)*

Department of Physics and Electronic Engineering, Nanjing Xiaozhuang University, Nanjing 211171, China
**Corresponding author: senlinyan@163.com*

Received October 1, 2014; accepted January 28, 2015; posted online March 10, 2015

Nonlinear dynamics in an optoelectronic delayed feedback semiconductor laser and its application in sensing are studied. We analyze the theories of stability and period of the laser. A route to quasi-periodic bifurcation or a stochastic state from stability is numerically analyzed by shifting the feedback level. The induced dynamics are found to be in one of four distributions (stable, periodic pulsed, period-three pulsed, and undamping oscillating). An external injection into the laser results in the process being more or less the opposite with the conventional optical injection cases. Based on this process or the dynamic regimes, we present a modeling of the incoherent detection sensor using the nonlinear period-one characteristic of the laser. The sensor discriminates the injection light variation as a sensing signal via detecting the behaviors from the period-one laser.

OCIS codes: 040.5160, 140.5960, 190.3100.
doi: 10.3788/COL201513.040401.

Semiconductor lasers can exhibit instability behaviors when additional freedoms are introduced to the lasers. A semiconductor laser due to optical feedback or external injection light can generate an unstable or a chaotic pulse[1–4]. Compared to these lasers, an optoelectronic laser system is much more reliable and flexible using electrical control[5–8]. Also, it is an indefinite-dimensional system with optoelectronic feedback and has high sensitivity to external injection variations. So it is of great importance for the complicated dynamical laser system in applications.

The richness of dynamics characteristics make lasers high invaluable for applications, e.g., for acoustics sensing, chemical sensing, gas spectroscopy, water flow sensing, lidar, sensing network[9–17], and so on. Chow and Wieczorek presented a chaotic laser sensor system for remote sensing[9]. Ji *et al.* presented a chaotic laser microwave–photonic sensor system for remote water-level monitoring[12]. A tunable chaotic fiber laser was used to realize a single-fiber link of the identical fiber Bragg grating sensor[13].

In the present work, we analyze nonlinear dynamics behaviors to find four distributions, such as stable, periodic pulsed, period-three pulsed, and undamping oscillating, and present a novel sensor, the basic idea based on sensing with one of its nonlinear dynamics regimes, such as "period-one" characteristic operation, conducive to a cyclic pulse[5–8]. The proposed idea of the sensing is based on a strong dependence of the amplitude induced in the period-one pulse. We demonstrate that a small variation of injection into the laser will induce an obvious shift in amplitude of the period-one pulse or state such that effective sensing can be achieved. The proposed system may be applicable for high-resolution real-time analysis, e.g., gas sensing, humidity detection, and lidar.

Dynamics in the optoelectronic feedback laser is described as a function of the feedback level, where the subsequent text lists the laser parameters. Results are summarized, where we find four zones, namely:

(1) stable zones, the dynamics in the system shifts to reach a stable state;
(2) undamped relaxation oscillations zones, where the laser shows stochastic fluctuations after period-one and period-three behaviors[3–5];
(3) self-pulsation zones, where the behavior of the laser oscillates periodically; these zones will be used in the context of sensing reference regimes where we find that a small injection into the laser results in an obvious diversification away from the period-one state;
(4) period-three zones, where the laser output shows three series of pulses.

The distributions of the found zones are different from those of the other systems[5–9]. An external injection into the laser results in the opposite process difference from the conventional optical injection cases. A novel sensor is presented and analyzed based on the qualitative changes in dynamical behaviors (periodic bifurcations or instabilities) exhibited by the laser subjected to an external signal.

A semiconductor laser was found to have sensitivity to optoelectronic feedback while the laser shows a lot of nonlinear oscillations, such as instability and undamping behaviors[5–8]. Figure 1 illustrates a delayed optoelectronic feedback semiconductor laser. A fixed dc source drives the laser to generate output. Then the lasing transmits to a photodetector to be exchanged into a photocurrent; the amplified photocurrent is fed back to generate the laser. In the transversions, the laser is induced to show some complicated behaviors. We can describe the system by[1,2,5–8]

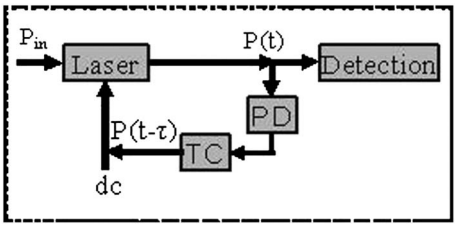

Fig. 1. Sketch of sensing setup showing the reference laser with optoelectronic delay feedback $P(t-\tau)$; dc, bias current; $P_{\rm in}$, injected signal, consisting of incoherent contribution; PD, photodetector; TC, delay time controller.

$$\frac{dP}{dt} = \left[g(N-N_{\rm th}) - \frac{1}{\tau_p}\right]P(t), \tag{1a}$$

$$\frac{dN}{dt} = J[1+\rho P(t-\tau)/P_u] - \frac{N}{\tau_s} - g(N-N_{\rm th})P(t), \tag{1b}$$

where P is the lasing amplitude and N is the active region carriers. P_u is the referenced optical amplitude. ρ is the feedback factor and τ is the delayed time. τ_s is the carriers lifetime. τ_p is the photon lifetime. g is the linear gain coefficient. $N_{\rm th}$ is the carrier density at transparency. J is the drive current density. Laser parameters are $N_{\rm th}=2.018\times10^{24}\,{\rm m}^{-3}$, $g=8.4\times10^{-13}\,{\rm m}^3{\rm s}^{-1}$, $\tau_s=2.02\,{\rm ns}$, $\tau_p=1.927$ ps, $J=1.2N_{\rm th}/\tau_s$, and the active volume $V=1.2\times10^{-16}$ m^{-3}.

At first, dynamics in the laser will be analyzed. Unmoving point (P_0, N_0) in Eq. (1) is obtained by

$$\left[g(N_0-N_{\rm th}) - \frac{1}{\tau_p}\right]P_0 = 0, \tag{2a}$$

$$J[1+\rho P_0/P_u] - \frac{N_0}{\tau_s} - g(N_0-N_{\rm th})P_0 = 0. \tag{2b}$$

We obtain the stable state for N_0 and P_0

$$P_0 = \frac{J - N_{\rm th}/\tau_s - 1/g\tau_p\tau_s}{\tau_p - J\rho/P_u}, \tag{3a}$$

$$N_0 = N_{\rm th} + 1/g\tau_p. \tag{3b}$$

The parameter ρ decides the stable output P_0. We adopt the following approximation

$$P = P_0 + \delta P e^{-\lambda t}, \qquad N = N_0 + \delta N e^{-\lambda t}, \tag{4}$$

where λ is the characteristic value. Substitute them into Eq. (1), we obtain

$$\frac{d^2}{dt^2}\delta P + \left(\frac{1}{\tau_s} + gP_0\right)\frac{d}{dt}\delta P + gP_0\left(\frac{J\rho}{P_u}e^{-\lambda\tau} - \frac{1}{\tau_P}\right)\delta P = 0, \tag{5}$$

the associated characteristic equation of which is obtained by

$$\lambda^2 - \left(\frac{1}{\tau_s} + gP_0\right)\lambda + gP_0\left(\frac{J\rho}{P_u}e^{-\lambda\tau} - \frac{1}{\tau_P}\right) = 0, \tag{6}$$

if $j\omega$ ($\omega > 0$) is a root of Eq. (6), only when ω satisfies

$$\omega^2 + gP_0\left(\frac{J\rho}{P_u}\cos\omega\tau - \frac{1}{\tau_P}\right) = 0, \tag{7a}$$

$$\left(\frac{1}{\tau_s} + gP_0\right)\omega + gP_0\sin\omega\tau = 0. \tag{7b}$$

Given these results, let $\omega^2 = y$; after some algebra, we obtain

$$y^2 + (K^2r_R^2 - 2\omega_R^2)y + \omega_R^4 - K^2g^2P_0^2 = 0, \tag{8}$$

where $\omega_R = \sqrt{gP_0/\tau_p}$, $r_R = (1/\tau_s + gP_0)$, and $K = J\rho/P_u$. Let $b = (K^2r_R^2 - 2\omega_R^2)$ and $c = \omega_R^4 - K^2g^2P_0^2$.

From Eq. (8), we obtain

$$y = \frac{-b \pm \sqrt{b^2-4c}}{2}. \tag{9}$$

Adopting the suitable parameters, let Eq. (9) have two positive roots. Suppose that the two positive roots as $\omega_k = \sqrt{y_k}$ where $k = 1, 2$. From Eq. (7b), we obtain

$$\sin\omega_k\tau = -\frac{r_R\omega_k}{gP_0}, \tag{10a}$$

$$\tau_k = \frac{1}{\omega_k}\left[\arcsin\left(-\frac{r_R\omega_k}{gP_0}\right) + 2n\pi\right], \tag{10b}$$

where $n = 0, 1, 2\ldots$. When the roots of Eq. (7) have a pair of purely imaginary $\pm i\omega_k$, periodic bifurcation may result. From Eq. (9), the value P_0 or the parameter ρ decides behavior in the laser.

Under the cases of $P_u = 0.1$ and $\tau = 1$ ns, we present a bifurcation diagram in Fig. 2 for the case of without external injection, where horizontal coordinates are divided into 100 equal slices and 50 equal slices for Figs. 2(a) and 2(d), respectively. Figures 2(a) and 2(d) indicate roughly a route to quasi-periodic bifurcation or a stochastic state from stability with the feedback level, where bifurcation occurs about $\rho = 0.06$. Figure 3 describes dynamic behaviors and dynamic regimes of the laser. Figure 3(a) illustrates the laser exhibiting a stable state for $\rho = 0.05$ after 25 ns where the laser performs a damping relaxation oscillation. The damping time is related to the term $1/\tau_s + gP_0$ when $\rho \ll 1$. The value of $1/\tau_s + gP_0$ is added by the positive feedback; it takes a long time for the laser to exhibit a stable state. The first dynamic regime is found from $\rho = 0$ to 0.055, where the laser exhibits a stable state

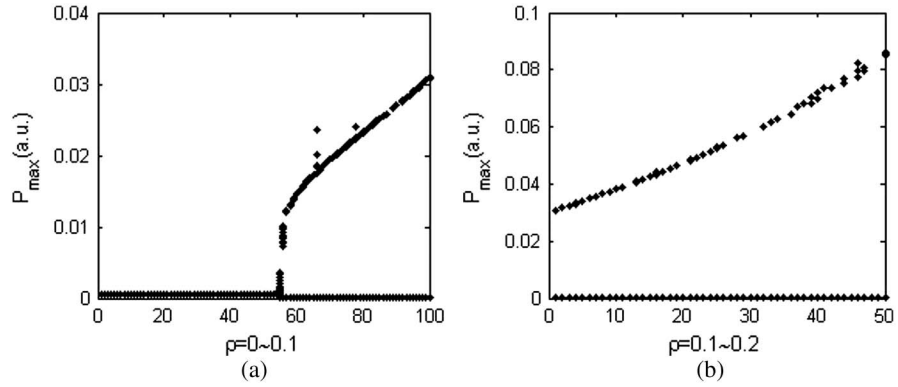

Fig. 2. Bifurcation diagram with the feedback levels. (a) $\rho = 0$–0.1; (b) $\rho = 0.1$–0.2.

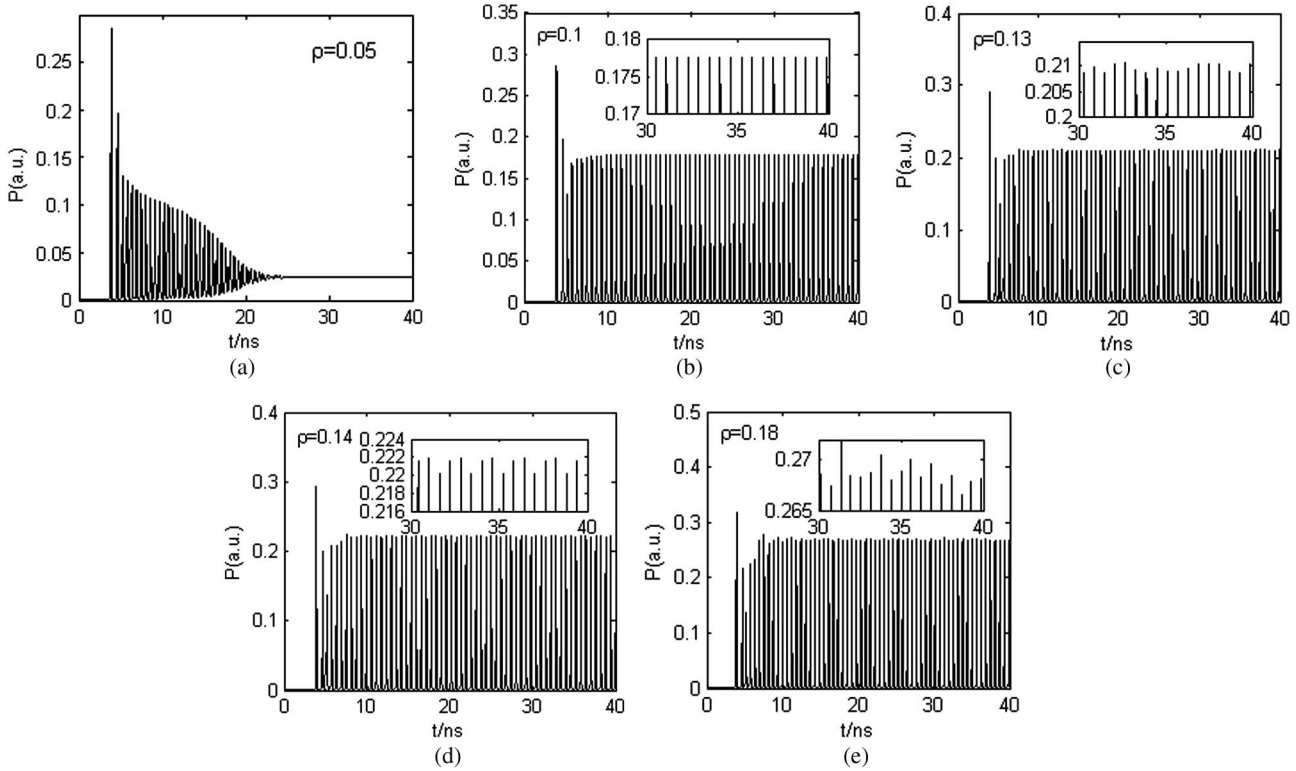

Fig. 3. Dynamics distributions; (a) stable, $\rho = 0.05$; (b) periodic pulsing, $\rho = 0.1$; (c) different undamping oscillating, $\rho = 0.14$; (d) period-three pulsing, $\rho = 0.13$; (e) different undamping oscillation, $\rho = 0.18$.

a long time after adding the feedback level. Next, the periodic oscillation regime is found from $\rho = 0.06$ to 0.12 where the laser exhibits periodic behavior, which implies that the laser emerges from bifurcation. Figure 3(b) shows a periodic behavior for $\rho = 0.1$ where the laser behavior oscillates with undamping relaxation and it produces a pulse cycle at 1.7 GHz after 10 ns. The relaxation time is found to be related to the term $(1/\tau_s + gP_0) - gP_0 J\rho\tau/P_u$ when the laser is supposed to relax at the main mode. The third dynamic regime exhibits some unstable behaviors when $\rho = 0.13$; the laser generates undamping oscillation [Fig. 3(c)]. The fourth dynamic regime is investigated to induce the laser to generate some period-three behaviors when $\rho = 0.14$; it takes 20 ns before the laser exhibits period-three states in Fig. 3(d) because the second modes of the laser are excited with the high feedback level. The fifth dynamic regime is investigated to illustrate that the laser shows stochastic fluctuations when $\rho \geq 0.15$. When $\rho = 0.18$, the laser generates undamping oscillation in Fig. 3(e). The induced dynamics are found to be in four distributions: stable, periodic pulsed, period-three pulsed, and undamping oscillating.

The infinite-dimensional system is sensitive to optical variations. We adopt the system as a reference laser to detect an external light variable. Self-pulsation zones in the laser will be used in sensing reference regimes where we find that a small injection into the period-one state is conducive to a strong shift in the laser.

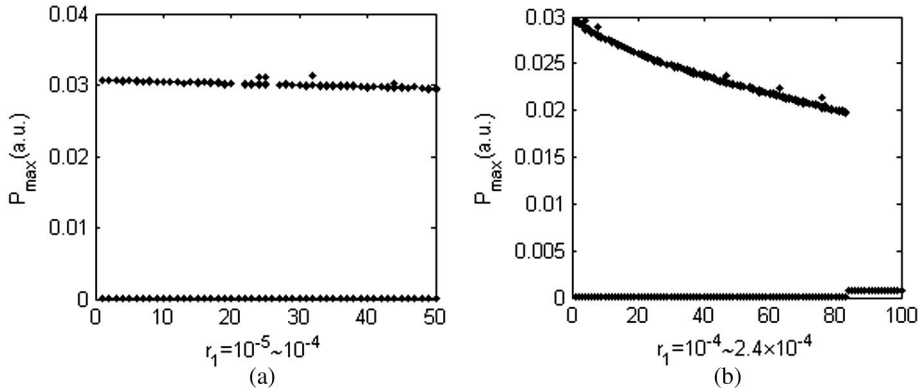

Fig. 4. Bifurcation diagram with the injection levels. (a) $r_1 = 10^{-5}$ to 10^{-4}; (b) $r_1 = 10^{-4}$ to 2.4×10^{-4}.

A sensing system model is now introduced. When external incoherent light is injected into the reference laser, the right-hand term in Eq. 1(a) is added by kP_{in}/τ_L, where the feedback factor k is written as $k = (1 - r_0^2)r_1/r_0$; r_0 and r_1 are the amplitude reflectivities of the laser exit facet and the external reflector, and τ_L is the round-trip time in the laser cavity, taking $\tau_L = 8$ ps. In numerical analysis, we take $r_0 = 0.556$ and vary r_1 to shift the injection level. We give results with respect to different injection levels.

When the optical injection is present, other unsightly dynamic behavior occurs in the laser and there is a strong change in the period-one state. The laser output switches to a stable state with increasing injection strength, and evolves from stochastic fluctuations into period-one and, finally, a stable state. The process is more or less the opposite those of the conventional optical injection cases. By analyzing this process or the dynamic regimes, we achieve the system sensing.

When $r_1 = 10^{-6}$, the laser still exhibits periodic behavior. The small injection cannot affect laser dynamics.

When $r_1 = 10^{-5}$, other unsightly dynamic behavior occurs in the laser and the injection results in changing the period-one state into stochastic fluctuations. We present a bifurcation diagram in Fig. 4 for the case of external injection, where horizontal coordinates are divided into 50 equal slices and 100 equal slices for Figs. 4(a) and 4(b), respectively. Figs. 4(a) and 4(b) illustrate roughly a route to stability from a quasi-period or stochastic state with the injection level, where bifurcation ends or stability occurs at about $r_1 = 0.0022$. Figures 5–7 describe dynamic behaviors of the laser. Figures 5(a) and 5(b) show stochastic fluctuations for $r_1 = 10^{-5}$ and $r_1 = 5 \times 10^{-5}$. We find unstable dynamic behaviors to be present from $r_1 = 10^{-5}$ to $r_1 = 9 \times 10^{-5}$ and enhancement of stochastic fluctuations with large parameter r_1.

When $r_1 = 10^{-4}$, period-two dynamic behavior is induced in the laser and the injection changes from the period-one state into the period-two state shown in Fig. 6(a). When $r_1 = 10^{-3}$, another period-two dynamic behavior results [Fig. 6(b)]. We find period-two dynamic behaviors to be present form $r_1 = 10^{-4}$ to $r_1 = 0.0021$ and reduction of period-two state fluctuations with a large value of the parameter r_1.

When $r_1 \geq 0.0022$, dynamic behavior is controlled at a stable state by the injection. Now, the period-one state in the reference laser is induced to be in a stable state. In this regime, Fig. 7(a) shows a stable state for $r_1 = 0.0022$. When $r_1 = 10^{-2}$, it takes 12 ns for dynamic behavior to be guided at a stable state shown in Fig. 7(b). We find

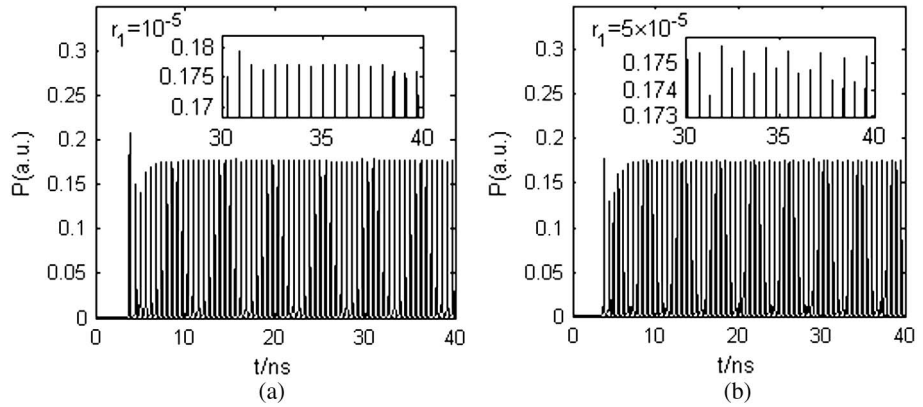

Fig. 5. Stochastic fluctuations (a) $r_1 = 10^{-5}$; (b) $r_1 = 5 \times 10^{-5}$.

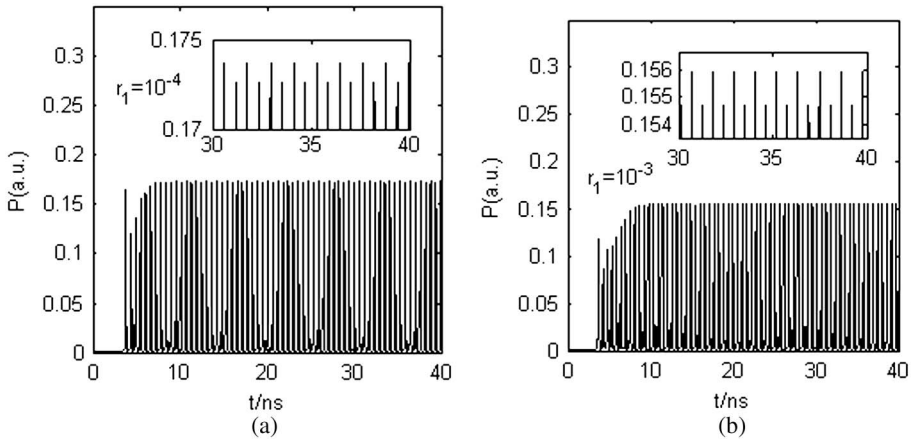

Fig. 6. Period-two behaviors; (a) $r_1 = 10^{-4}$; (b) $r_1 = 10^{-3}$.

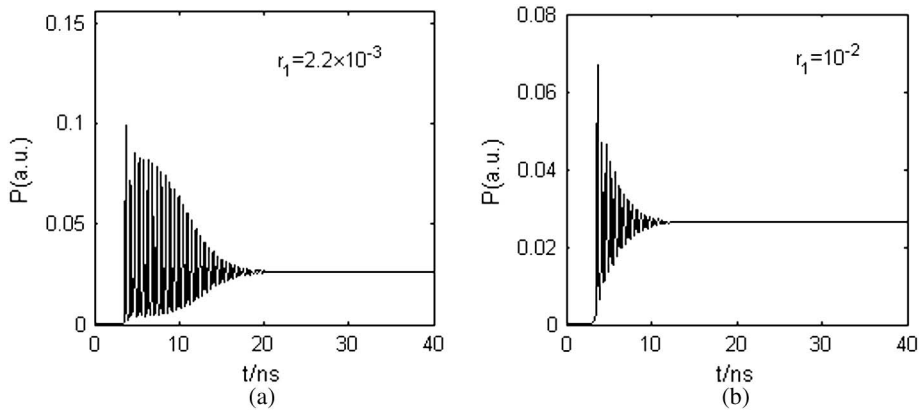

Fig. 7. Stable states; (a) $r_1 = 2.2 \times 10^{-3}$; (b) $r_1 = 10^{-2}$.

that dynamic behavior is quickly guided to a stable state and stable output is added when a large value of r_1 is applied.

In conclusion, utilizing a reference injection level between $r_1 = 10^{-5}$ and $r_1 = 9 \times 10^{-5}$, we can analyze stochastic fluctuation variables for detecting or sensing. When we take a reference injection level between $r_1 = 10^{-4}$ and $r_1 = 0.0021$, period-two dynamic behavior is analyzed for detecting or sensing. When we take a reference injection level higher than 0.0022, dynamic behavior time and stable output is analyzed for detecting or sensing.

A theory of dynamics in the laser due to the optoelectronic delayed feedback is elucidated. A route to periodic bifurcation from stability is numerically simulated while the induced dynamics in four distributions are found: stable, periodic pulsed, period-three pulsed, and undamping oscillating. By analyzing this process or the dynamic regimes under the cases of the injection, we present a modeling of the incoherent detection sensor using period-one distribution to discriminate the injection light variety as a sensing signal via detecting the behaviors from the period-one distribution. The proposed system may be applicable for high-resolution real-time analysis, e.g., gas sensing, humidity detection, and lidar.

References

1. C. G. Lim, S. Iezekiel, and C. M. Snowden, IEEE J. Quantum Electron. **37**, 699 (2001).
2. S. L. Yan, Opt. Eng. **50**, 044202 (2011).
3. J.-G. Wu, L.-J. Zhao, Z.-M. Wu, D. Lu, and X. Tang, Opt. Express **21**, 23358 (2013).
4. S. Xiang, W. Pan, L. Zhang, A. Wen, L. Shang, H. Zhang, and L. Lin, Opt. Commun. **324**, 38 (2014).
5. S. Tang and J. M. Liu, IEEE J. Quantum Electron. **37**, 329 (2001).
6. S. L. Yan, J. Opt. Commun. **30**, 20 (2009).
7. S. L. Yan, Opt. Laser Technol. **44**, 1351 (2012).
8. T. Deng, G. Q. Xia, L. P. Cao, J. G. Chen, X. D. Lin, and Z. M. Wu, Opt. Commun. **282**, 2243 (2009).
9. W. W. Chow and S. Wieczorek, Opt. Express **17**, 7491 (2009).
10. E. Lacot, R. Day, and F. Stoeckel, Phys. Rev. A **64**, 043815 (2001).
11. T. Gong, Y. Wang, L. Kong, H. Li, and A. Wang, Chin. J. Lasers **36**, 2426 (2009).
12. Y. Ji, M. Zhang, Y. Wang, P. Wang, A. Wang, Y. W. H. Xu, and Y. Zhang, Int. J. Bifurcation Chaos **24**, 1450032 (2014).
13. F. Wang, L. Zhang, L. Yang, and Y. Liu, Acta Opt. Sin. **34**, 0806006 (2014).
14. H. Arellano-Sotelo, A. V. Kir'yanov, Y. O. Barmenkov, and V. Aboites, Opt. Laser Technol. **43**, 132 (2011).
15. X. Wang, F. Liu, A. Liu, B. Fan, K. Cui, X. Feng, W. Zhang, and Y. Huang, Chin. Opt. Lett. **12**, 010602 (2014).
16. T. Hu and X. Sun, Chin. Opt. Lett. **11**, 070602 (2013).
17. W. Diao, X. Zhang, J. Liu, X. Zhu, Y. Liu, D. Bi, and W. Chen, Chin. Opt. Lett. **11**, 072801 (2013).